

A DOSIMETRY STUDY OF PORTABLE X-RAY FLUORESCENCE IN VIVO METAL MEASUREMENTS

Aaron J. Specht,¹ Xinxin Zhang,² Benjamin D. Goodman,³ Ed Maher,¹
Marc G. Weisskopf,¹ and Linda H. Nie²

Abstract—Portable x-ray fluorescence devices have grown in popularity for possible metal exposure assessment using in vivo measurements of bone and toenail. These measurements are accompanied by a small radiation dose, which is typically assessed by radiation safety committees to be minimal. However, an understanding of precise dose under different instrument conditions is still needed. This study set out to do a thorough investigation of the exact dose measurements using optically stimulated dosimeters, thermoluminescent dosimeters, and simulation with a Monte Carlo N-Particle transport code to assess the skin and total-body effective dose typical of portable x-ray fluorescence devices. We showed normal linear relationships between measurement time, x-ray tube current, and radiation dose with the device, and we showed a second order polynomial relationship with increasing voltage and radiation dose. Dose was quantified using thermoluminescent dosimeters, optically stimulated dosimeters, and simulations, which gave similar dose estimations. Skin dose for a standard 50-kV, 40- μ A measurement for bone and toenail in vivo was 48.5 and 28.7 mSv, respectively, according to simulation results. Total-body effective dose was shown as 3.4 and 2.0 μ Sv for in vivo bone and toenail measurements, respectively, for adults using the portable x-ray fluorescence device.

Health Phys. 116(5):590–598; 2019

Key words: dose assessment; exposure, radiation; metal, trace; radiation effects

INTRODUCTION

PORTABLE X-RAY fluorescence (XRF) devices are being used more frequently for in vivo measurements to assess metal exposures in populations. The risks associated with the radiation exposure from these low-energy x-ray tubes are minimal, but since they are used in population studies, a more

thorough review of the radiation exposure would be appropriate to fully consider the radiation exposures associated with the use of portable x-ray fluorescence devices.

Metal exposure assessment has been performed for decades using x-ray fluorescence. Previous devices for x-ray fluorescence measurements used radionuclides as a source to stimulate the characteristic x-ray emissions (Chettle et al. 1991). In particular, the ¹⁰⁹Cd radionuclide K-shell XRF device for lead measurement had well-characterized radiation dose, which was summarized in a previous study (Nie et al. 2007). The radiation dose associated with portable XRF measurements has not been characterized as accurately and thoroughly. Only one previous study has explored the radiation dose with measurements using thermoluminescent dosimeters (Nie et al. 2011). However, it was quickly found after optimization of the device that the x-ray tube current used for this measurement was not optimal, and changes in x-ray tube settings were proposed for future studies, and further changes are likely in the future to optimize for different metal or tissue measurements (Specht et al. 2014).

Portable XRF presents a unique problem since the device uses a modifiable source, which can be used on different tissues to measure different biomarkers of exposure. Changes to the source or tissue examined would result in changes to the radiation dose and radiosensitive organs in the measurement. In this study, we measured radiation dose from a portable XRF and identified the changes in dose with different x-ray tube voltage, current, and filtration when doing bone lead and toenail metal measurements.

MATERIALS AND METHODS

Portable XRF device

We used a Thermo Fisher XL3t GOLDD+ portable XRF device for this study (Thermo Fisher Inc., Billerica, Massachusetts, US). The device is typically used commercially for mining and soil measurements but has been investigated for use in metal exposure assessment in vivo. This study focuses on in vivo uses and the associated radiation dose. This same x-ray system has been used in previous studies measuring bone in vivo for strontium and lead, and

¹Harvard T.H. Chan School of Public Health Boston, MA; ²School of Health Sciences, Purdue University West Lafayette, IN; ³Saint Francis Medical Center, Cape Girardeau, MO.

The authors declare no conflicts of interest.

For correspondence contact Aaron Specht, 655 Huntington Avenue, Building 1, Rm 1402, Boston, MA 02115, or email at aspecht@hsph.harvard.edu.

(Manuscript accepted 8 August 2018)

0017-9078/19/0

Copyright © 2018 Health Physics Society

DOI: 10.1097/HP.0000000000000971

for measuring toenails in vivo for mercury and manganese (Specht et al. 2014, 2016, 2017a and b; Zhang et al. 2017). For this study, we used variable voltage, current, and filters from the device, which we note in the results for our measurements. The maximum power output of the x-ray tube was 2 W.

Standard phantoms

Soft tissue and bone equivalent phantoms were used in this study to determine the dose for in vivo bone measurements. Lucite (Lucite International UK, Ltd., Southampton, UK) plate phantoms were used to simulate soft tissue over bone by placing the Lucite under the flat surface of the bone phantoms in increments of 1 mm up to 5 mm of Lucite thickness. These Lucite plates were found to be an acceptable phantom for soft tissue in our previous study (Specht et al. 2014). Cylindrical phantoms with a flat base for measurements were made of plaster of paris and were used to simulate bone. These measurements were made from the flat base of the phantom.

Toenail phantoms were made to test in vivo measurements of toenail metals. Standard phantoms for toenails were made using epoxy resin with added salt to standardize the attenuation coefficients, similar to prior work (Roy et al. 2010; Zhang et al. 2017). For the dose assessment we used toenail with 0.6 and 1.3 mm to determine the influence of toenail thickness on the radiation dose.

Optically stimulated luminescence dosimetry system

For this study we used a Landauer InLight MicroStar Optically Stimulated Luminescence Dosimeter (OSLD) reader (Landauer, Glenwood, Illinois, US). This system has been used in studies of similar surface dose measurements in clinical practice (Yusof et al. 2015). The system was calibrated using standard OSLDs obtained from Landauer. Two calibrations were completed, one for low-dose response (3 OSLDs between 0.10 to 10 mGy) and one for high-dose response (3 OSLDs between 0.01 to 15 Gy). The measurements of calibration OSLDs were made nine times to ensure accuracy, and it was found that there was <2% change between readings, which fit the qualifications for clinical use of OSLD measurements according to TG-191 American Association of Physicists in Medicine (AAPM) recommendations (AAPM 2017). The OSLDs used for dose measurements were found to be accurate within 10% with repeated measures of the same x-ray settings, which is primarily due to a higher background dose present in many of the OSLDs. Error from these measurements are represented in the figures as a measure of the error identified in our repeatability tests during measurements. We used these measurements to get a sense of the characteristic relationships between the portable XRF radiation dose and different situations, and we did not expect a calibration of these OSLDs to produce quantified results within clinical-level accuracy from this study.

We measured the radiation dose from a variety of settings and setups of phantoms. We first used a number of different geometries with the OSLDs in order to find the maximal dose. We measured the dose using x-ray tube settings 50 kV, 40 μ A, and an iron and silver filter changing the time from 0.5, 1, 2, 3, and 4 min. We also did tests changing the current from 40 μ A to 30, 20, and 10 μ A, while keeping the other settings the same; then doing the other iterations, changing the voltage to 40 kV and changing the current from 50 μ A to 40, 30, 20, and 10 μ A with filtration and time constant. We did tests using aluminum and titanium, molybdenum and iron, and iron and silver filtration, which could prove to be useful for certain in vivo measurements.

Finally, we did dose measurements using 50 kV, 40 μ A, and silver and iron filtration for bone and skin measurements. We used 0, 1, 3, and 5 mm of skin thickness to induce scatter. Then we used bare bone with no skin phantoms, 3-mm skin with bone, and 5-mm skin with bone. We attempted to estimate surface bone dose by placing the OSLDs between the skin and bone phantom at 1, 2, 3, and 5 mm of skin. Lastly, we did tests of entrance and exit dose to toenail phantoms with thicknesses of 0.6 and 1.3 mm using both 50-kV, 40- μ A and 40-kV, 50- μ A x-ray tube settings with silver and iron filtration.

Thermoluminescent dosimeters

Thermoluminescent dosimeters (TLDs) were used in this study for further validation of the dose readings. TLD 700 chips were used in this study, since the dose associated with XRF is purely from photons. The TLDs were read using a Harshaw TLD 4000 reader (Harshaw Partnership, Solon, Ohio, US). The TLDs were calibrated against known exposures from a gamma irradiator at Purdue University. A Gammacell 220 (Nordion International Inc., Ottawa, Canada) containing a ^{60}Co radionuclide source with known exposure rates. Each TLD used in this study was separately irradiated for doses of 0, 25, 50, 75, 125, 250, 500, and 1,000 mR (the units in which the source is calibrated for exposure), which were each measured three times to ensure the accuracy of the TLDs. The combined calibration curves of the TLDs produced a line with a correlation R^2 of 0.995, which gave us confidence in the quantification and accuracy of results obtained using these TLDs.

We first used a number of different geometries for measurement to find the maximal dose for the TLD measurements. The portable XRF comes standard with a camera, which can identify items placed in the field of view of the x-ray tube, which we used for verification of dosimeter placement consistency. We measured these dosimeters with x-ray tube settings of 50 kV, 40 μ A with an iron and silver filter for 3 min under soft tissue and bone phantoms, and 40 kV, 50 μ A with an iron and silver filter for 3 min under toenail, Lucite soft tissue phantoms, and bone phantoms.

Finally, we used a grid pattern of four TLD chips to average over and better recreate our normalized skin area of 1 cm^2 (this approach approximated an area of $\sim 0.8 \text{ cm}^2$).

Monte Carlo simulations

We used the Monte Carlo simulation program, Monte Carlo N-Particle (MCNP) transport code, in our study, which was developed by Los Alamos National Lab and distributed by the Radiation Safety Information Computational Center. This software has recently been updated to more accurately depict interactions at lower energies, using its default database for interaction cross sections. This includes Doppler broadening effects and all interactions observed in XRF. In a previous study, we validated the use of this simulation to accurately simulate the output from the x-ray tube of the exact portable XRF used in this study (Specht et al. 2017b). There was less than 9% difference between simulated and experimental spectral from that study. MCNP gives us the ability to set unique materials, densities, geometries, and sources in order to reproduce an experimental setup and, in the case of this study, to reproduce the dose of in vivo measurements. Previous studies have similarly used MCNP to estimate dose to patients in clinical settings (Yoriyaz et al. 2001). We used the same x-ray tube simulation as our previous study but added in skin, bone, or toenail based on the specifications for our study. We did simulations to reproduce the in vivo bone measurements and give estimates for bone and skin dose. We also did simulations of toenail in vivo measurements to look at skin dose below the toenail. The bone and skin composition and densities were taken from International Commission on Radiation Units and Measurements (ICRU) Report 44 (ICRU 1989), and the toenail composition was taken from Rutherford and Hawk (1907). The simulation included a 40-cm-long leg, which was used in full for energy deposition measurements in the total-body effective dose calculations. For skin dose, only a 1-cm^2 voxel of the skin in the maximal area of exposure was used for dose measurements. In the calculations of

dose, we used the number of particles that would have been used in the x-ray tube based on the amperage and a time of 3 min, which should make the measurements equal to those with TLDs and OSLDs with 3-min exposures.

Total-body effective dose calculations

We calculated total-body effective dose for the bone measurement using the simulation to get total skin and total-surface bone dose from the simulated 40-cm-long leg. For the toenail measurements, we assumed the same area of exposure except with the added attenuation of toenail. The dose from the bone was assumed to be all-surface dose, since the penetration depth of x rays from the portable XRF would only be $\sim 0.5 \text{ mm}$ into the bone. We used a simulation with skin (skin thickness 5 mm) and bone tissue 40 cm in length (bone radius 1.25 cm) to ensure we captured the full dose of any scattering that occurred. We approximated the total-body bone surface using different values for 5-y-old, 10-y-old, and adult females and males. From Specker et al. (2001), 5-y-old male and female bone area was taken to be 950 and 935 cm^2 , respectively. For adult males and females, we used a 2013 Centers for Disease Control (CDC) report on total-body bone area with values $1,385$ and $1,399 \text{ cm}^2$ for 10-y-olds and $2,272$ and $1,918 \text{ cm}^2$ for adults (Looker et al. 2013). We assumed the density of bone was 1.7 , 1.75 , and 1.8 g cm^{-3} for 5-y-old, 10-y-old, and adult, respectively, as taken from the table on page 37 of International Commission on Radiological Protection (ICRP) 70 (ICRP 1995). For skin areas we used 0.78 , 1.12 , and 1.90 m^2 for 5-y-old, 10-y-old, and adult, respectively (ICRP 2002). We also included a comparison of total-body effective dose with different tissue thickness values of 1 , 3 , and 5 mm .

RESULTS

OSLD results

Fig. 1 shows the linear dose relationship with measurement times using 50 kV , $40 \mu\text{A}$, and iron and silver filtration.

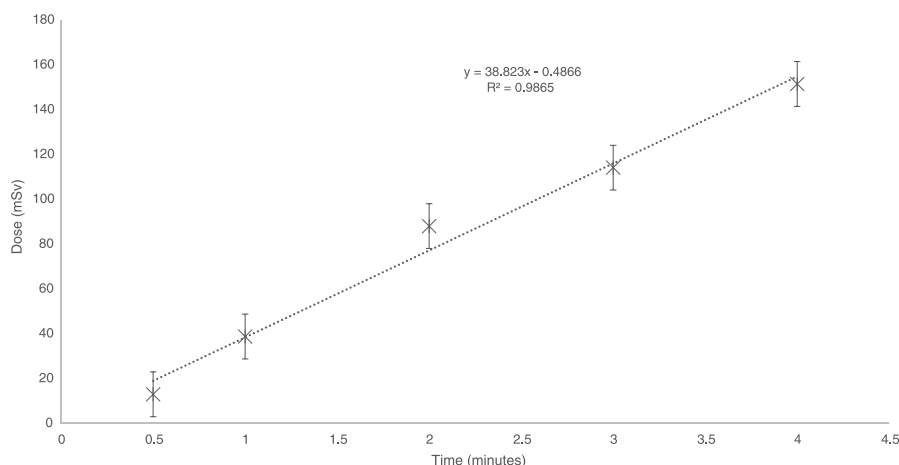


Fig. 1. Radiation entrance skin dose (0.2 cm^2) changes with different measurement times using 50 kV , $40 \mu\text{A}$, and silver and iron filtration.

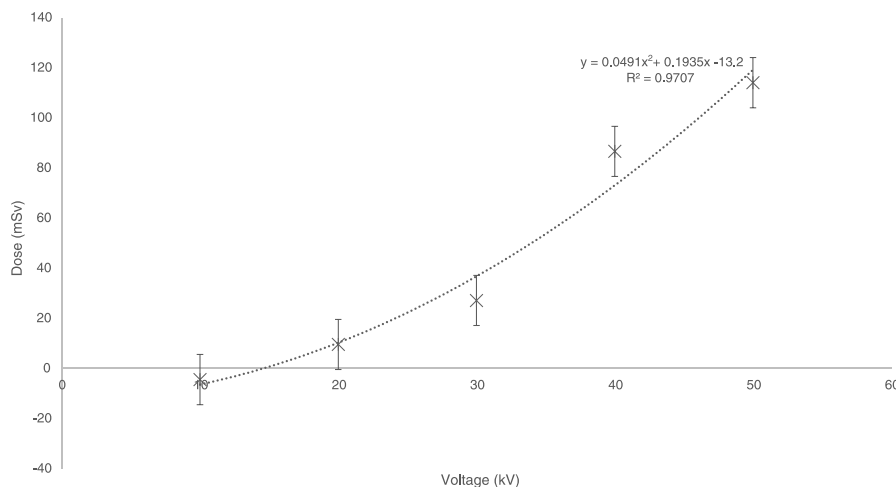


Fig. 2. Radiation entrance skin dose (0.2 cm^2) changes with different x-ray tube voltage settings using $40 \mu\text{A}$ and silver and iron filtration.

Figs. 2, 3, and 4 show the significant nonlinear relationship between dose and changes in voltage of the portable XRF device with constant $40 \mu\text{A}$ and iron and silver, molybdenum and iron, and aluminum and titanium filtration. Fig. 5 shows the linear relationship between measured dose and current keeping 40 kV and the iron and silver filtration constant. Finally, Fig. 6 shows the relationship between surface bone dose and skin thickness, which decreased slightly with increasing skin thickness. Increasing the skin thickness over the dosimeters, which would potentially increase scatter, did not increase the dose measured by the OSLD. The 1-cm^2 skin dose measurements using aluminum and titanium, molybdenum and iron, and iron and silver filtration at 50 kV , $40 \mu\text{A}$, and 3 min were 224.7 , 49.0 , and 103.7 mSv , respectively.

Thermoluminescent dosimeter measurements

We took measurements using TLDs to look at the radiation dose for in vivo measurements of toenail and bone with two separate measurements for each. The results for

these measurements are summarized in Table 1. The average result from a grid of 4 TLD chips ($\sim 0.8 \text{ cm}^2$ area) arranged over the irradiated area during a bone and toenail measurement changed the dose to 48.8 and 43.3 mSv , respectively. The differences in dose quantification are explained in the Discussion section.

Simulation dose measurements

We used the simulation to calculate the dose of the bone surface and skin, which would be the only components that would receive radiation dose from in vivo measurements using the portable XRF. Using this, we can then calculate total-body effective dose for our measurements. The results for the measurements of skin dose and total-body effective dose for bone and toenail measurements are shown in Table 2. The leg was 40 cm in length to capture all scatter, but for the skin dose only a 1-cm^2 voxel was used to determine skin dose. For total-body effective dose, we used energy deposition in skin and bone surface, which we averaged over the previously mentioned total-body skin and bone surface

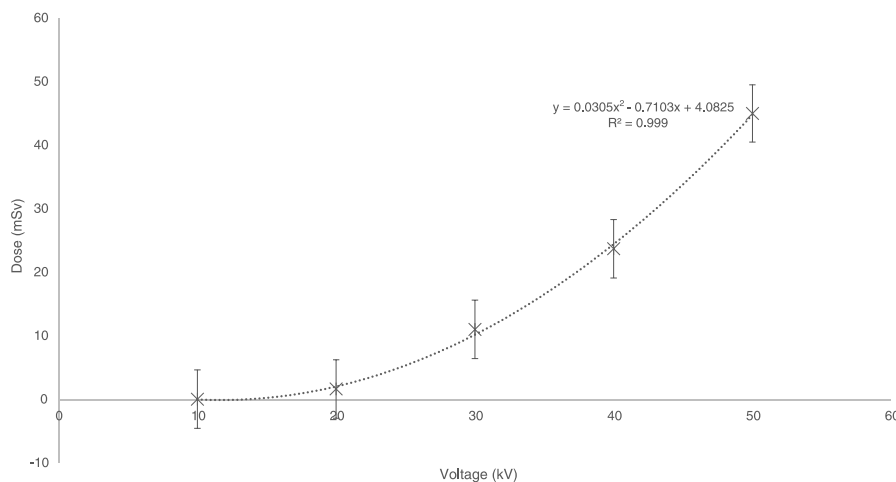


Fig. 3. Radiation entrance skin dose (0.2 cm^2) changes with different x-ray tube voltage settings using $40 \mu\text{A}$ and molybdenum and iron filtration.

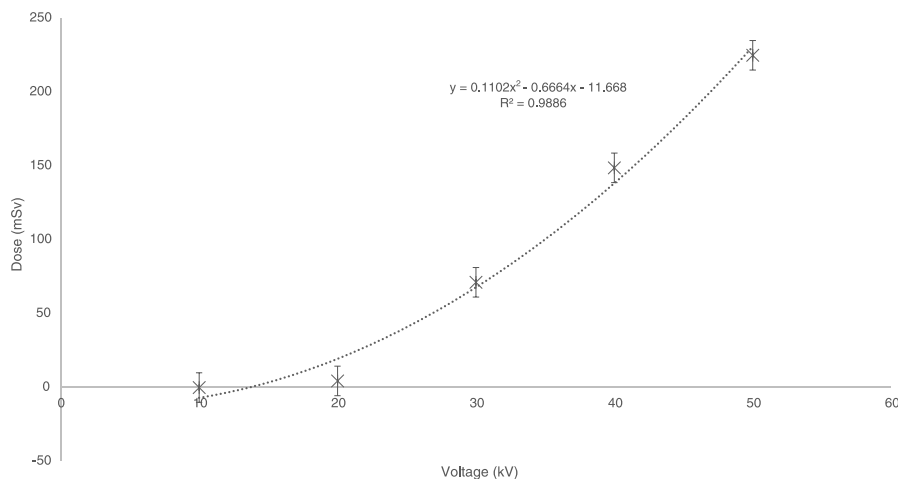


Fig. 4. Radiation entrance skin dose (0.2 cm^2) changes with different x-ray tube voltage settings using $40 \mu\text{A}$ and aluminum and titanium filtration.

areas to arrive at the final values. We assume all the dose going to the bone is surface dose, surface bone and skin are the only contributing factors to total-body effective dose in bone measurements, and the skin dose is the only contributing factor to total-body effective dose from the toenail measurements. We conservatively used female average values for 5-y-old, male for 10-y-old, and female for adult calculations to report the highest possible dose. The simulation resulted in a bone dose averaged over the simulated leg (40-cm long and 1.25-cm radius) of 2.2, 2.2, and 2.1 mSv for 5-y-old, 10-y-old, and adult, respectively. The simulated skin dose averaged over the total leg was $1.1 \mu\text{Sv}$. Changing the tissue thickness and bone surface dose resulted in a total-body effective dose of 3.4, 3.7, and $4.3 \mu\text{Sv}$ at 5, 3, and 1 mm tissue thickness, respectively.

In vivo dose measurement comparisons

Table 3 shows a side-by-side comparison of the skin dose estimates made by measuring the dose with simulation, TLDs, and OSLDs, and their respective volume differences.

DISCUSSION

This study determined radiation doses from using portable XRF devices for in vivo measurements in order to determine the suitability for such use. We found the total-body effective dose delivered by the device in a 3-min measurement to be reasonable and skin dose to be at a level higher and more concentrated than typical of diagnostic exams but far from any deterministic radiation risk. We demonstrated the relationship of the radiation dose from the device with increasing time, amperage, and voltage in the x-ray tube, and the effect of different filtration on the radiation dose. Finally, we used simulations to determine and compare the experimental measures of skin and total-body effective dose measurements.

One limitation of our experimental results from the study is accounting for slight geometry changes in the measurements. The x-ray tube aperture is quite small, and for this reason, it was potentially easy to place a TLD or OSLD in a spot that did not reflect the highest potential dose. To combat this issue, we initially did measurements with

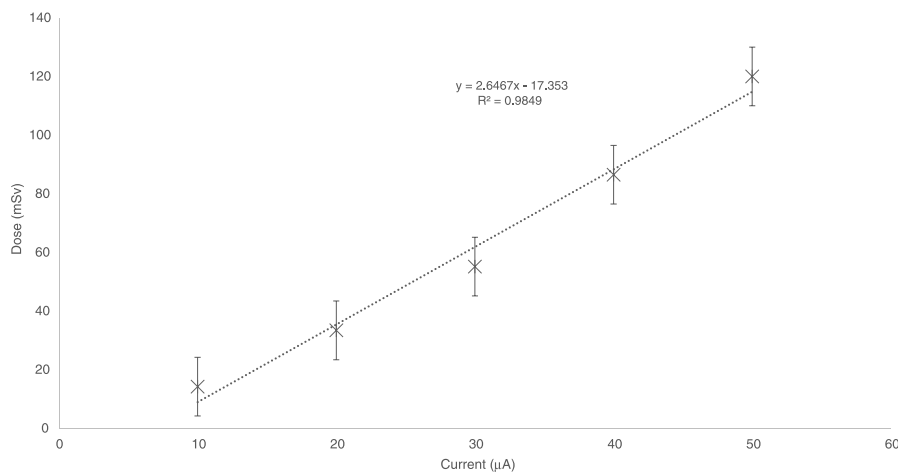


Fig. 5. Radiation entrance skin dose (0.2 cm^2) changes with different x-ray tube current settings using 40 kV and silver and iron filtration.

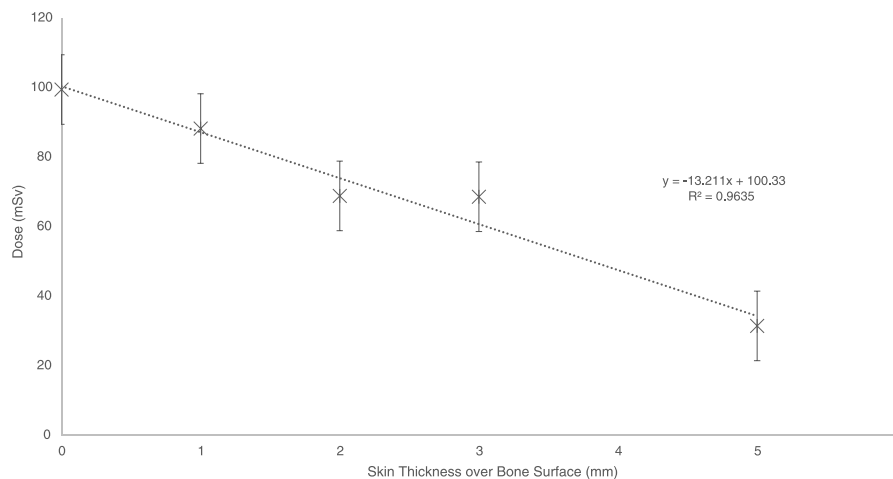


Fig. 6. Bone surface dose changes with increasing thickness of skin over bone using 50 kV, 40 μ A, and silver and iron filtration.

multiple TLDs and OSLDs to determine the geometry with the maximal dose. This maximal dose geometry is what we attempted to replicate for the other measurements as part of the study. However, it is hard to determine whether or not the maximal dose was captured for every measurement, but the simulation results would not have had this same issue.

Using our phantom measurements, we were able to identify dose distribution changes with skin thickness. As expected, bone dose would decrease with increasing skin thickness over bone, but the results show a linear relationship. Over the small thickness increases shown with in vivo measurements of about 5 mm, the exponential interaction with attenuation is approximately the same as a linear relationship. Using National Institute of Standards and Technology (NIST) values for the attenuation coefficient of skin, we can determine what the approximate dose changes should be with increases in skin thickness assuming a perfectly collimated beam, and at 5 mm of skin thickness the bone surface dose should be 65.9 mSv. We show a value of 31.4 mSv for the bone surface dose at 5 mm of skin thickness. This difference is likely due to the x-ray tube source collimation being imperfect, and the beam likely spreads over a larger area with increasing distance, similar to an inverse square effect.

There was an observable difference in dose quantification between TLD, OSLD, and simulation measurements. This is mainly attributable to the varying averaged volumes for the doses for each of these measurements, which is

evidenced by our results using a grid of four TLDs, which gave results in line with the estimated volume changes. In the singular TLD and OSLD measurements, we are not averaging over a true 1-cm² area but are measuring about 0.2 cm². Since the x-ray tube aperture of the portable XRF is actually smaller than 1 cm², it is likely most of the dose from entrance skin exposure to the x rays will be more concentrated than this initial area limit. Another potential reason for the quantification differences is in the calibration procedure for TLD and OSLD measurements. The calibration was done on standard TLD or OSLD chips, which were under almost uniform exposure. Since the dose from the portable XRF is highly concentrated at one area of the dosimeter, as mentioned above, it could affect the reading of the TLD and OSLD. In addition, the OSLDs were calibrated from standard OSLDs obtained from the manufacturer, but ideally they should be calibrated to include additional corrections due to fading, angular dependences, and beam quality that could all play a role in the differences identified between the results. However, the main use of the OSLDs in our study was to study the relationships of the radiation dose with changes in the in vivo measurement, which should be consistent regardless of quantification issues.

The phantoms used as a proxy for skin, bone, and toenails in our experimental setup were not able to perfectly represent the radiation interactions of real skin, bone, or toenails. Lucite as a skin phantom was shown to be spectrally equivalent to cadaver skin in a previous study, but even

Table 1. Skin dose to 0.2 cm² from in vivo measurements of bone and toenail.

Measurement	Dose measurements (mSv)	
	5-mm skin with bone	1.3-mm toenail
1	73.9	67.9
2	60.2	61.7

Table 2. Skin, bone, and total-body effective dose from bone and toenail portable XRF measurements.

	Total-body effective dose (μ Sv)	
	Bone measurement	Toenail measurement
5-y-old	7.4	4.4
10-y-old	4.9	2.9
Adult	3.4	2.0

Table 3. Skin dose measurements from in vivo portable XRF measurements using different measurement techniques.

	Dose estimates (mSv)			
	TLD (0.2 cm ²)	TLD (~0.8 cm ²)	OSLD (0.2 cm ²)	Simulation (1 cm ²)
Bone measurement	73.9	48.8	103.7	48.5
Toenail measurement	67.9	43.3	111.7	28.7

considering this there are slight differences in attenuation and density. Similarly, the density and attenuation of plaster of paris is not the same as bone, as discussed in an in-depth calibration study (Da Silva and Pejovic-Milic 2017). The toenails were made to match attenuation coefficients of the characteristic x rays of specific metals of interest between 5–11 keV, as discussed in previous studies, but the attenuation coefficients will vary as the energy changes from the energies of interest which will also change the scattering dose (Roy et al. 2010; Zhang et al. 2017). These differences will likely reflect an increase in the radiation dose from scatter of around 10 to 20% for the phantom measurements in comparison to true in vivo measurements due to the increased scatter cross sections for the phantoms. Considering that the majority of the dose likely arises from direct interaction with the initial x-ray beam and the use of phantoms showed minimal increase in dose, we can accept these measurements and relationships to be slightly more conservative than true in vivo dose measurements. The simulation used accurately depicted human compositional and density data and included a life-size human leg for total-body effective dose quantification, so simulation results should be the most accurate in terms of comparisons to radiation dose experienced in a true in vivo measurement.

Using the total-body effective dose, we can estimate the risk of radiation-induced cancers. The increased risk for cancer and other inheritable effects from radiation has been found to be 5% per sievert of total-body effective dose (ICRP 2007). Given the doses we found from the 3-min portable XRF measurement, this would mean a 0.000004%, 0.000003%, and 0.000002% increased risk of cancer for 5-y-olds, 10-y-olds, and adults, respectively (ICRP 2007).

Deterministic effects from skin dose have been shown to occur for doses in excess of 2 Gy according to ICRP Publication 85; the portable XRF skin dose is 400 times less than this (ICRP 2000). This 2-Gy limit for skin doses is typically assigned assuming a uniform dose to an area; however, studies in radiation therapy patients have shown that when doses are limited to small areas, stem cells migrate from surrounding unaffected skin to repopulate the areas affected by DNA damage (von Essen 1969; Withers 1967). More recent studies have shown this to increase the resiliency of normal tissues by up to a factor of 4, which in the use of the portable XRF would further

reduce the unlikely possibility of deterministic skin damage due to the small radiation beam used for measurements (Narayanasamy et al. 2017).

Given the minimal skin dose and total-body effective dose associated with these measurements, even measurement times as high as 10 min could be considered while maintaining a reasonable limit for exposure. The limit for total-body effective dose to any member of the public set by US Nuclear Regulatory Commission's (NRC) 10 CFR 20.1301 is at 1 mSv y⁻¹ (US NRC 2018), which is 100–300 times more than given in a single 3-min measurement from our device.

The total-body effective dose measurements shown in Table 2 were taken as the highest dose considering differences in sex. We had sex-specific data only for total-body bone area and were not able to find sex-specific data for skin area. The dose difference between males and females was minor, with the greatest difference in the adult calculation of total-body effective dose of 2.9 μ Sv for males and 3.4 μ Sv for females. For 10-y-old males, doses were higher due to lower total bone area, since females typically have more growth earlier than males due to puberty. Almost all of the total-body effective dose arose from the absorbed dose in the surface of the bone.

The surface bone dose decreases slightly in relation to increases in the overlying tissue thickness, and detection accuracy for in vivo metal measurements decreases with increasing skin thickness. For in vivo measurement, typically there is a tradeoff between accuracy of the measurement and radiation dose (Specht et al. 2014). As the surface bone dose decreases, so does the signal that arises from the bone, which in turn increases the uncertainty of the metal quantification measurement. In our previous study, we found 3-min measurements with 50 kV and 40 μ A would achieve reasonable detection limits for populations with skin thicknesses less than 5 mm (Specht et al. 2014). In further application of the device, we found this to be a less reasonable assumption for all populations (Specht et al. 2016). With the results shown here, it seems that longer measurement times of up to 10 min would be feasible while maintaining acceptable radiation dose limits. This would reduce the detection limit by a factor of the square root of the increase in time or current, which in this case would be a decrease of a factor 1.8.

However, we need to make sure the increased measurement times would not be overexposing those with low tissue thickness in order to capture a greater proportion of the population. Our results indicate that the dose change for individuals with lower soft tissue thicknesses is relatively minor with an increase of about 0.8 μ Sv total-body effective dose from 5-mm to 1-mm tissue thickness for a 3-min measurement. The detection limit change over this tissue thickness difference is much more drastic with a detection limit

of 11.0 and 1.8 ppm for 5- and 1-mm tissue thickness, respectively (Specht et al. 2014). This demonstrates that the primary limiting factors of the detection limit of the measurement come from a combination of the absolute efficiency of the detector, which decreases with the inverse square law from increasing tissue thickness and the added attenuation from soft tissue thickness. The inverse square drop off with distance is a result of the characteristic x-ray production in the bone being isotropic, which will greatly decrease the efficiency of the detector with increasing distance from the characteristic x rays arising in the bone. The added attenuation is a larger factor for the outgoing x-ray signal, since the initial x-ray beam is of higher average energy than the characteristic x-ray signal. Thus, the x-ray signal would have a higher interaction cross section and probability of attenuation with increases in tissue thickness. Although our results indicate the radiation dose and total number of interactions creating signal in the bone will change, that relationship is almost linear over the range of tissue thicknesses in the general population and will have limited impact on increases in the detection limit in comparison to the changes induced by the inverse square effect and outgoing signal attenuation.

CONCLUSION

This study looked at the radiation dose administered while taking in vivo metal measurements with a standard 2-W silver x-ray tube. We showed normal linear relationships between measurement time, x-ray tube current, and radiation dose with the device, and we showed a second order polynomial relationship with increasing voltage and radiation dose. Dose was quantified using TLDs, OSLDs, and simulations, which gave similar dose estimations. Skin dose for a standard 50-kV, 40- μ A measurement of bone and toenails in vivo was 48.5 and 28.7 mSv according to simulation results. Total-body effective dose was shown as 3.4 and 2.0 μ Sv for in vivo bone and toenail measurements for adults using the portable XRF device with a 3-min measurement.

Acknowledgments—This work was supported by the National Institute of Environmental Health Science (NIEHS) R21 grant R21ES024700. The authors would like to thank the Radiological and Environmental Management (REM) Department at Purdue University and the Environmental, Health, and Safety (EH&S) health physics staff for the support and equipment in the study.

REFERENCES

American Association of Physicists in Medicine. Recommendations on the clinical use of luminescent dosimeters (TG191). Task Group No. 191—AAPM. AAPM Committee Tree [online]. 2017. Available at https://www.aapm.org/org/structure/default.asp?committee_code=TG191. Accessed 20 March 2018.

Chettle DR, Scott MC, Somerville LJ. Lead in bone: sampling and quantitation using K x-rays excited by ^{109}Cd . *Environ Health Perspect* 91:49–55; 1991.

Da Silva E, Pejovic-Milic A. Calibration of the ^{125}I -induced x-ray fluorescence spectrometry-based system of in vivo bone strontium determinations using hydroxyapatite as a phantom material: a simulation study. *Physiol Meas* 38(6), 1077–1093; 2017. DOI:10.1088/1361-6579/aa63d3.

International Commission on Radiation Protection. Basic anatomical and physiological data for use in radiological protection—the skeleton. Oxford: Pergamon Press; ICRP Publication 70; 1995.

International Commission on Radiation Protection. Avoidance of radiation injury from medical interventional procedures. Oxford: Pergamon Press; ICRP Publication 85; 2000.

International Commission on Radiation Protection. Basic anatomical and physiological data for use in radiological protection: reference values. A report of age- and gender-related differences in the anatomical and physiological characteristics of reference individuals. Oxford: Pergamon Press; ICRP Publication 89; 2002.

International Commission on Radiation Protection. The 2007 recommendations of the International Commission on Radiological Protection. Oxford: Pergamon Press; ICRP Publication 103; 2007.

International Commission on Radiation Units and Measurements. Tissue substitutes in radiation dosimetry. Oxford: Oxford University Press; ICRU Report 44; 1989.

Looker AC, Borrud LG, Hughes JP, Fan B, Shepherd JA, Sherman M. Total body bone area, bone mineral content, and bone mineral density for individuals aged 8 years and over: United States, 1999–2006. *Vital Health Stat* 11:1–78; 2013.

Narayanasamy G, Zhang X, Meigooni A, Paudel N, Morrill S, Maraboyina S, Penagaricano J. Therapeutic benefits in grid irradiation on tomotherapy for bulky, radiation-resistant tumors. *Acta Oncol* 56:1043–1047; 2017. DOI 10.1080/0284186X.2017.1299219.

Nie H, Chettle D, Luo L, O'Meara J. Dosimetry study for a new in vivo x-ray fluorescence (XRF) bone lead measurement system. *Nuclear Instr Meth Phys Res B* 263: 225–230; 2007.

Nie H, Sanchez S, Newton K, Grodzins L, Cleveland RO, Weisskopf MG. In vivo quantification of lead in bone with a portable x-ray fluorescence system—methodology and feasibility. *Phys Med Biol* 56:N39–51; 2011. DOI 10.1088/0031-9155/56/3/N01.

Roy CW, Gherase MR, Fleming DE. Simultaneous assessment of arsenic and selenium in human nail phantoms using a portable x-ray tube and a detector. *Phys Med Biol* 55:N151–159; 2010. DOI 10.1088/0031-9155/55/6/N02.

Rutherford T, Hawk P. Comparative chemical composition of the hair of different races. *J Biol Chem* 3:459–489; 1907.

Specht AJ, Lin Y, Weisskopf M, Yan C, Hu H, Xu J, Nie LH. XRF-measured bone lead (Pb) as a biomarker for Pb exposure and toxicity among children diagnosed with Pb poisoning. *Biomarkers* 21:347–352; 2016. DOI 10.3109/1354750X.2016.1139183.

Specht AJ, Mostafaei F, Lin Y, Xu J, Nie LH. Measurements of strontium levels in human bone in vivo using portable x-ray fluorescence (XRF). *Appl Spectrosc* 71:1962–1968; 2017a. DOI 10.1177/0003702817694383.

Specht AJ, Weisskopf M, Nie LH. Portable XRF technology to quantify Pb in bone in vivo. *J Biomarkers* 2014:398032; 2014. DOI 10.1155/2014/398032.

Specht AJ, Weisskopf MG, Nie LH. Theoretical modeling of a portable x-ray tube based KXRF system to measure lead in bone. *Physiol Meas* 38:575–585; 2017b. DOI 10.1088/1361-6579/aa5efe.

- Specker B, Johannsen N, Binkley T, Finn K. Total body bone mineral content and tibial cortical bone measures in preschool children. *J Bone Mineral Res* 16:2298–2305; 2001.
- US Nuclear Regulatory Commission. Dose limits for individual members of the public. Washington, DC: US NRC; 10 CFR 20.1301; 2018.
- von Essen CF. Radiation tolerance of the skin. *Acta Radiol Ther Phys Biol* 8:311–330; 1969.
- Withers HR. The dose-survival relationship for irradiation of epithelial cells of mouse skin. *Br J Radiol* 40:187–194; 1967. DOI 10.1259/0007-1285-40-471-187.
- Yoriyaz H, Stabin MG, dos Santos A. Monte Carlo MCNP-4B-based absorbed dose distribution estimates for patient-specific dosimetry. *J Nucl Med* 42:662–669; 2001.
- Yusof FH, Ung NM, Wong JHD, Jong WL, Ath V, Phua VCE, Heng SP, Ng KH. On the use of optically stimulated luminescent dosimeter for surface dose measurement during radiotherapy. *PLOS ONE* 10:e0128544; 2015. DOI 10.1371/journal.pone.0128544. Available at <https://journals.plos.org/plosone/article?id=10.1371/journal.pone.0128544>. Accessed 8 March 2018.
- Zhang X, Specht AJ, Weisskopf MG, Weuve J, Nie LH. Quantification of manganese and mercury in toenail in vivo using portable x-ray fluorescence (XRF). *Biomarkers* 23:154–160; 2017. DOI 10.1080/1354750X.2017.1380082.

